JOURNAL OF MATERIALS SCIENCE 30 (1995) 1561–1564

Thermal properties and devitrification behaviour of $(1+x)CaO\cdot(1-x)MgO\cdot 2SiO_2$ glasses

A. COSTANTINI, F. BRANDA, A. BURI
Dipartimento di Ingegneria dei Materiali e della Produzione, Università "Federico II", Napoli, Italia

The thermal properties (glass transformation, T_g, and softening, T_s, temperatures), the crystalline phases formed during heating in a differential thermal analysis (DTA) apparatus, the kinetic parameters and the mechanism of the devitrification process, of glasses of the system diopside–wollastonite were investigated. The substitution of CaO by MgO induces an increase in T_g and the crystal growth activation energy, E_c; this is probably linked to the greater coordination number of Ca^{2+} ions with respect to the Mg^{2+} ions. The substitution of CaO by MgO lowers the nucleation rates of the diopside phase; wollastonite solid solution nuclei form whose growth appears to leave a glassy matrix in which diopside formation is inhibited. Only surface nucleation was observed, but, in finely powdered samples, which soften and efficiently sinter before devitrifying, surface nuclei behave as bulk nuclei. When bulk crystallization occurs, the Avrami parameter m was found to be 2 for all glasses, except the diopside one, for which $m=3$.

1. Introduction

CaO and SiO_2 in the molar ratio $CaO/SiO_2 \approx 1$ are the basic components of bioactive glasses and glass-ceramics [1, 2]. The present work is part of a more general study of the effect on thermal properties and devitrification behaviour of equimolar substitution, in the glass of composition $CaO\cdot SiO_2$, of CaO by divalent or trivalent oxides. This paper reports the effect of the substitution of MgO for CaO. From the composition of the glasses, wollastonite and diopside are expected to form on devitrification. They are the same as the main crystalline phases that form in the glass-ceramics obtained from natural rocks, mostly basalt, tuff, granite with the addition of dolomite, limestone and nucleating agents [3].

2. Experimental procedure

Glasses of compositions expressed by the following formula $(1+x)CaO\cdot(1-x)MgO\cdot 2SiO_2$, $0 \leq x \leq 1.0$, were prepared by melting analytical grade reagents, $MgCO_3$, $CaCO_3$ and SiO_2 in a platinum crucible in an electric oven for 4 h, in the temperature range 1400–1600 °C. The melts were quenched by plunging the bottom of the crucible into cold water. Thermal analysis was carried out using a Netzsch differential scanning calorimeter (DSC) model 404M on about 50 mg powdered samples at various heating rates, 2–20 °C min^{-1}. Finely (63–90 μm) and coarsely (315–500 μm) powdered samples were used. Powdered Al_2O_3 was used as reference material.

Devitrified samples were analysed in a computer-interfaced X-ray (CuK_α) powder diffractometer (XRD) using a Philips diffractometer model PW1710, with a scan speed of 1 ° min^{-1} using a built-in computer search program. The crystalline phases were identified by means of JCPDS cards.

3. Results

Figs 1 and 2 show the DTA curves at 10 °C min^{-1} heating rate, together with the derivative curve (DDTA) of one of them, for finely (63–90 μm) (Fig. 1) and coarsely (315–500 μm) (Fig. 2) powdered samples. When a glass is heated in a DTA apparatus, a slope change appears on the recorded curve when passing through the glass transition temperature range. The glass transformation temperature, T_g, can be defined and easily taken from the derivative curve, as indicated in Fig. 1. As can be seen, in many cases the first slope change in the glass transformation range is followed by a second one at a temperature lower than the onset of the devitrification exo-peak. In these cases the initially powdered samples were recovered from the DSC sample holders as porous bodies. Therefore, the second slope change is linked to the change in the thermal exchange coefficients when powders soften and sinter. The effect is much more pronounced in the case of the fine powders. The softening temperatures can be taken from the DSC curves, as indicated in Fig. 1. As can be seen from Fig. 3, T_g increases as the CaO content is increased. The same figure shows the plot of softening temperatures, T_s, versus composition.

Fig. 4 shows the X-ray diffraction patterns for samples from a DTA run stopped just after the exo-peak,

0022–2461

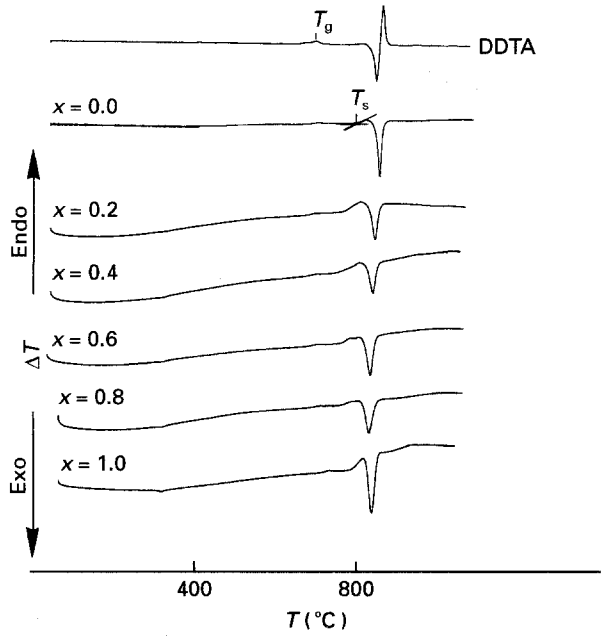

Figure 1 DTA and DDTA curves recorded at 10 °C min^{-1} heating rate on finely (63–90 μm) powdered samples.

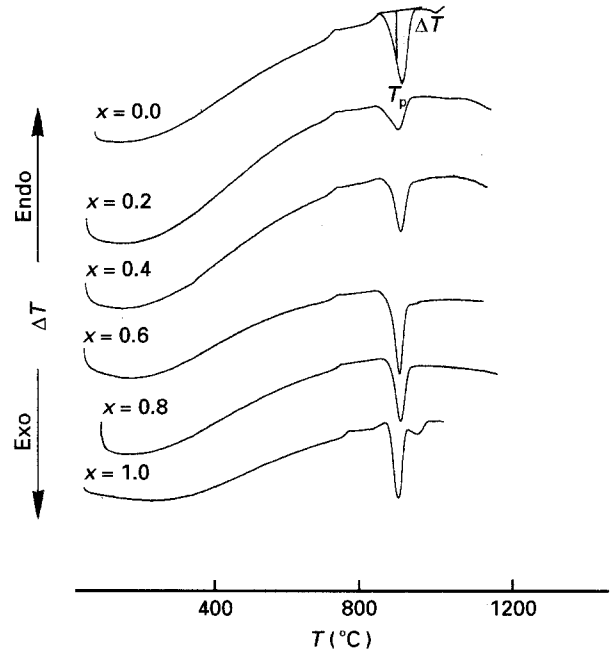

Figure 2 DTA curves recorded at 10 °C min^{-1} heating rate on coarsely (315–500 μm) powdered samples.

except for XRD pattern (b); this refers to the sample $1.2CaO \cdot 0.8MgO \cdot 2SiO_2$ heat treated for 10 h at 1100 °C. The lines in patterns (a) and (g), can be attributed to diopside (JCPDS card 11/654) and wollastonite (JCPDS card 29/372). The other diffraction patterns, except (b), show the same lines as are present in (g), but progressively shifted as the CaO is substituted by MgO. Therefore, wollastonite solid solution forms. In these patterns the lines of diopside are absent. Patterns (b) and (c) although referring to the same glass, are strikingly different. Pattern (b) shows lines of both diopside and wollastonite, as expected from the composition of the glass. It is worth pointing out that, on the contrary, when a sample of $1.2CaO \cdot 0.8MgO \cdot 2SiO_2$ is subjected to a DTA run

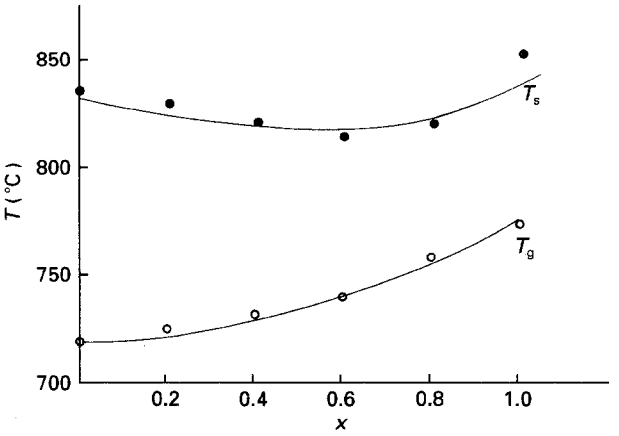

Figure 3 (○) Glass transformation temperature, T_g, and (●) softening temperature, T_s, versus composition.

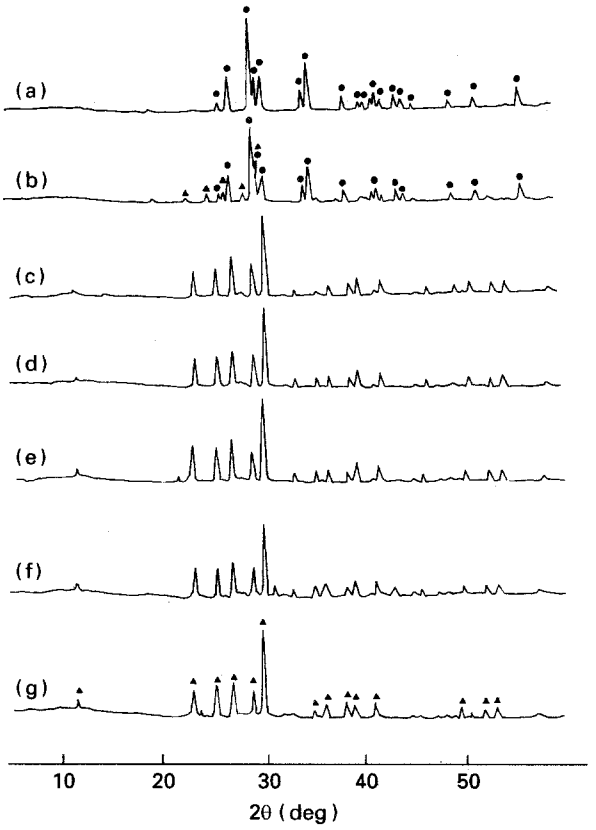

Figure 4 X-ray diffraction patterns after the DTA run: (a) $x = 0$; (c) $x = 0.2$; (d) $x = 0.4$; (e) $x = 0.6$; (f) $x = 0.8$; (g) $x = 1.0$; (b) $x = 0.2$ after 10 h at 1100 °C. (●) diopside (JCPDS card 11/654), (△) wollastonite (JCPDS card 29/372).

stopped after 10 h at 950 °C the same pattern is obtained as shown in (c). Therefore, the XRD results for samples from a DTA run are not consistent with the reported phase diagram [4], according to which wollastonite solid solution and diopside should form in all the intermediate glasses ($0.2 \leq x \leq 0.8$).

The non-isothermal devitrification was also studied. The kinetic parameters were determined by using the following equations

$$\ln \beta = -E_c/RT_p + \text{const} \quad (1)$$

$$\ln \Delta T = -mE_c/RT + \text{const} \quad (2)$$

Equations 1 and 2 can be derived from the well-known Equation [5, 6]

$$-\ln(1-\alpha) = AN/\beta^m \exp(-mE_c/RT) \quad (3)$$

were α is the degree of crystallization, N is the number of nuclei, A is a constant, β is the heating rate, and ΔT and T_p are the deflection from the base line and the peak temperature taken as indicated in Fig. 2; T is the temperature. As in inorganic glasses the devitrification exo-peak occurs in a temperature range higher than that of efficient nucleation [5], E_c is the crystal growth activation energy. The parameter m depends on the mechanism and morphology of crystal growth; it ranges from $m = 1$ for one-dimensional growth (or growth from surface nuclei) to $m = 3$ for three-dimensional growth [5, 6].

Equations 1 and 2 can be derived from Equation 3 by supposing: (1) α at the peak temperature is not dependent on the heating rate [7]; (2) ΔT is proportional to the instantaneous reaction rate [8, 9]; (3) in the initial part of the DTA crystallization peak, the change in the temperature has a much lower effect than α on ΔT [10].

Fig. 5 shows a plot of $\ln\beta$ versus $1/T_p$; straight lines were also obtained for the other glasses studied. In Figs 6 and 7 the plots of $\ln\Delta T$ (taken as indicated in Fig. 2) versus $1/T$ are reported for finely and coarsely powdered samples. According to Equations 1 and 2, straight lines were obtained. Their slopes allow, therefore, the E_c and mE_c values reported in Figs 8 and 9 to be evaluated. E_c slightly increases as CaO is substituted by MgO. As can be seen from Fig. 9, the mE_c values increase as the specific surface of the samples is increased. When comparing the values of E_c with mE_c

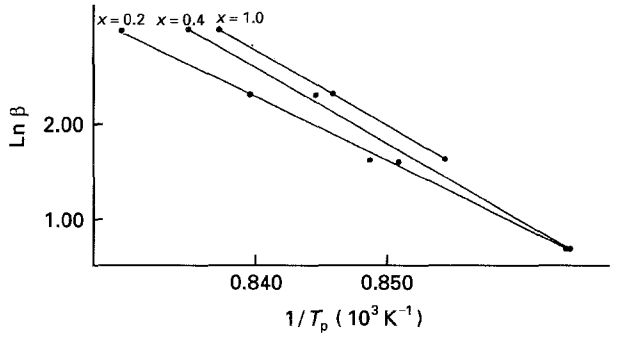

Figure 5 Plot of $\ln\beta$ versus $1/T_p$.

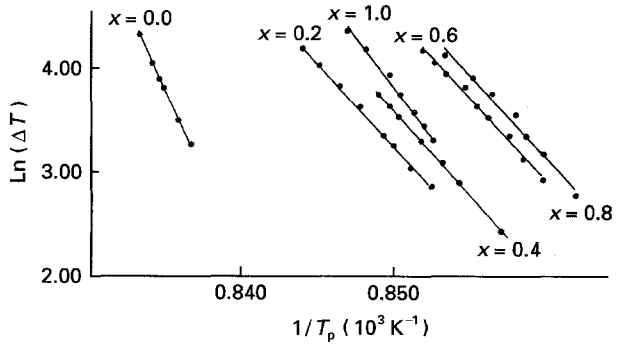

Figure 6 Plot of $\ln\Delta T$ versus $1/T$ relative to finely powdered samples (63–90 μm).

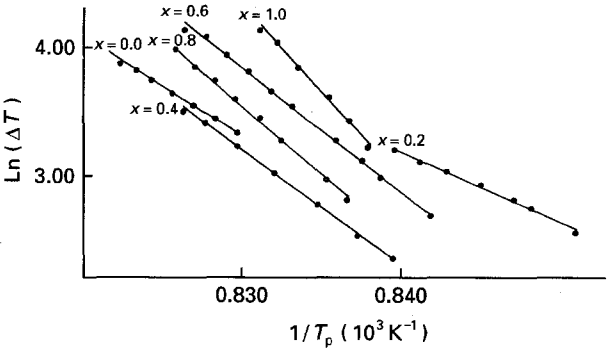

Figure 7 Plot of $\ln\Delta T$ versus $1/T$ relative to coarsely powdered samples (315–500 μm).

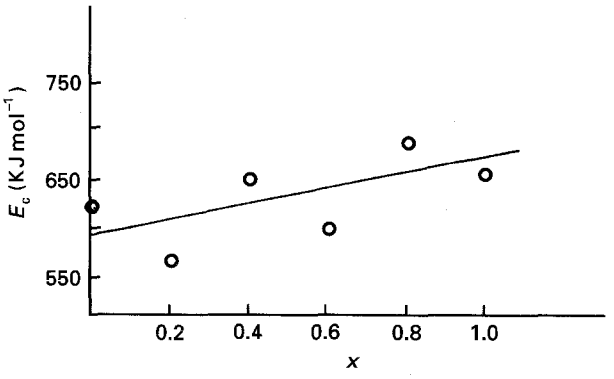

Figure 8 Activation energy for crystal growth, E_c, versus composition.

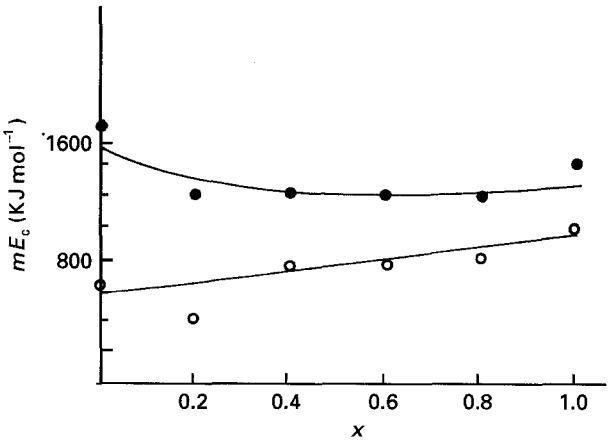

Figure 9 mE_c values versus composition for (●) finely powdered samples (63–90 μm), and (○) coarsely powdered samples (315–500 μm).

for the finely powdered samples, values of $m \approx 2$ are obtained for all the glasses of the studied system, except the diopside glass for which $m \approx 3$. In the case of coarse powdered samples, a value $m \approx 1$ is always obtained.

4. Discussion

The T_g increase, when CaO is substituted for MgO, can be explained by taking into account that, according to Ray [11], the glass transformation temperature depends on the density of covalent cross-linking and the number and strength of the cross-links between the cation and oxygen atoms. It is worth remembering

that CaO and MgO are reported to be modifier oxides and that in their pure oxides the coordination number of Ca^{2+} (n.c. = 8) is greater than that of Mg^{2+} (n.c. = 6) [12]. When CaO is substituted for MgO, the density of covalent cross-linking does not change, because the molar ratio O/Si is constant in the studied series; the T_g increase can, therefore, be ascribed to the greater coordination number of the Ca^{2+} ion with respect to Mg^{2+}. Taking into account that the crystal growth activation energy is usually equal to the viscous flow activation energy, the slight increase of E_c, when CaO is substituted for MgO, can also be explained as the result of the increased rigidity of the structure.

When examining the XRD results, it is useful to remember that when a glass is heated in a DTA apparatus, nucleation and growth occur separately [5]: nuclei form in the glass transformation range and grow in the temperature range of the exo-peak. The XRD results suggest that the substitution of CaO by MgO inhibits the formation of the nuclei of the diopside phase. On the contrary, wollastonite solid solution nuclei form. It is worth pointing out that a sample of the $x = 0.2$ glass heated in a DTA apparatus up to the exo-peak temperature and kept for 10 h at this temperature, gives the same XRD pattern as pattern (c) in Fig. 4. Therefore the comparison of patterns (b) and (c) suggests that the crystal growth of the previously formed nuclei leaves a glassy matrix of composition different from the diopside phase, in which diopside crystal formation is inhibited.

The mE_c values increase as the specific surface of the samples is increased. A similar result has been found when studying the non-isothermal devitrification of glasses obtained by substituting Y_2O_3 for CaO in the glass of composition $CaO \cdot SiO_2$ [13]. Usually the opposite result is obtained: the greater the specific surface the greater is the tendency to devitrify by growth from surface nuclei, so that m is progressively reduced to the value $m = 1$. In the case of $CaO \cdot MgO \cdot 2SiO_2$ [14], $CaO \cdot SiO_2$ [15], $1.4CaO \cdot (0.6/3)Y_2O_3 \cdot 2SiO_2$ [15] and $1.6CaO \cdot 0.4MgO \cdot 2SiO_2$ [15] glasses, scanning electron micrographs confirmed that nucleation preferentially occurs at the surface of the sample, but surface nuclei formed in the glass transformation range behave as bulk nuclei in finely powdered samples that efficiently sinter before devitrifying. This hypothesis is effective in explaining the devitrification behaviour of all the studied glasses. In fact, in the case of coarsely powdered samples that sinter poorly (see Figs 1 and 2), a value of $m \approx 1$ was obtained for all the glasses studied. On the contrary, in the case of finely powdered samples that sinter well before devitrifying, higher values of m were obtained. The value $m \approx 2$ for wollastonite agrees with the reported result that its crystals are often in the form of tablets [16]. The mechanism is consistent with the reported result that in diopside glass, surface nucleation preferentially occurs [17]. Otherwise, bulk crystallization of wollastonite is known only for glass-ceramics melted under strongly reduced conditions using slag as raw material with a metal sulphide [18].

5. Conclusions

1. When CaO is substituted by MgO, T_g and E_c increase as the result of the greater coordination number of the Ca^{2+} ion with respect to Mg^{2+}.

2. XRD patterns can be explained by admitting that, when CaO is substituted by MgO, nuclei of wollastonite solid solution preferentially form with respect to the diopside ones. Their growth leaves a glassy phase in which diopside formation is inhibited.

3. The homogeneous nucleation rates are very low; nevertheless surface nuclei can behave as bulk nuclei in powdered samples that sinter before devitrifying.

4. When bulk crystallization occurs the value $m = 2$ was found for all the studied glasses, except the diopside one, for which $m = 3$.

References

1. L. L. HENCH, *J. Am. Ceram. Soc.* 74 (1991) 1487.
2. T. KOKUBO, *Bol. Soc. Esp. Ceram. Vid.* (Proc. XVI International Congress on Glass, Vol. I) **31-C 1** (1992) 119.
3. Z. STRNAD, "Glass-Ceramic Materials" (Elsevier, Amsterdam, 1986) p. 110.
4. E. M. LEVIN, C. R. ROBINS and H. F. McMURDIE "Phase diagrams for Ceramists" (The American Ceramics Society, Columbus, OH, 1964) P. 211.
5. K. MATUSITA and S. SAKKA, *Bull. Inst. Chem. Res. Kyoto Univ.* **59** (1981) 159.
6. D. R. MacFARLANE, M. MATECKI and M. POULAIN, *J. Non-Cryst. Solids* **64** (1984) 351.
7. P. G. BOSWELL, *J. Thermal Anal.* **18** (1980) 353.
8. H. J. BORCHARDT and F. DANIELS, *J. Am. Chem. Soc.* **79** (1957) 41.
9. K. AKITA and M. KASE, *J. Phys. Chem.* **72** (1968) 906.
10. F. O. PILOYAN, I. V. RYABCHICA and O. S. NOVIKOVA, *Nature* **212** (1966) 1229.
11. N. H. RAY, *J. Non-Cryst. Solids* **15** (1974) 423.
12. H. RAWSON, "Inorganic Glass Forming Systems" (Academic Press, London, New York, 1967) p. 24.
13. A. COSTANTINI, F. BRANDA and A. BURI, *J. Eur. Ceram. Soc.*, in press.
14. F. BRANDA, A. COSTANTINI and A. BURI, *Thermochim. Acta* **217** (1993) 207.
15. F. BRANDA, A. COSTANTINI, A. BURI and A. TOMASI, *J. Thermal Anal.* **41** (1994) 1979.
16. A. N. WINCHELL and H. WINCHELL, "The microscopical characters of artificial inorganic substances: optical properties of artificial minerals" (Academic Press, New York, London, 1964) p. 291.
17. E. D. ZANOTTO, *J. Non-Cryst. Solids* **130** (1991) 217.
18. K. MAEDA, E. ICHIKURA, Y. NAKAO and S. ITO, *Bol. Soc. Esp. Ceram. Vid.* (Proc. XVI International Congress on Glass, Vol. 5) **31-C** (1992) 15.

Received 13 July 1993
and accepted 28 September 1994